JOURNAL OF GEOPHYSICAL RESEARCH, VOL. 105, NO. A9, PAGES 21,067–21,077, SEPTEMBER 1, 2000

Mini-Magnetospheric Plasma Propulsion: Tapping the energy of the solar wind for spacecraft propulsion

R. M. Winglee

Geophysics Program, University of Washington, Seattle

J . Slough and T. Ziemba

Department of Aeronautics and Astronautics, University of Washington, Seattle

A. Goodson

The Boeing Corporation, Seattle, Washington

Abstract. Mini-Magnetospheric Plasma Propulsion is a potentially revolutionary plasma propulsion concept that could enable spacecraft to travel out of the solar system at unprecedented speeds of 50 to 80 km s^{-1} or could enable travel between the planets for low power requirements of ~ 1 kW per 100 kg of payload and ~ 0.5 kg fuel consumption per day for acceleration periods of several days to a few weeks. The high efficiency and specific impulse attained by the system are due to its utilization of ambient energy, in this case the energy of the solar wind, to provide the enhanced thrust. Coupling to the solar wind is produced through a large-scale magnetic bubble or mini-magnetosphere generated by the injection of plasma into the magnetic field supported by solenoid coils on the spacecraft. This inflation is driven by electromagnetic processes, so that the material and deployment problems associated with mechanical sails are eliminated.

1. Introduction

Material from other stars can be measured in situ just beyond the heliopause, which represents the boundary between the solar wind and the interstellar wind [e.g., *Suess,* 1990]. This boundary is thought to be at ~140 ± 20 AU, with 1 AU = 1.5 x 10^8 km being the distance from the Sun to the Earth [e.g., *Baranov and Malama,* 1993, 1995; *Steinolfson et al.,* 1994; *Linde et al.,* 1998]. The solar wind itself moves out from the Sun with an average speed of 350 to 800 km s^{-1}, and on occasions even to 1000 km s^{-1} [e.g., *McComas et al.,* 1998] and experiences essentially no deceleration until the termination shock, which is at approximately 80 ± 10 AU. At this boundary, the solar wind flow changes from supersonic to subsonic. This deceleration is produced by interactions of the outflowing solar wind with reflected solar wind particles, transmitted interstellar particles, and neutrals from the interstellar medium.

Between ~35 to 1000 AU lies the Kuiper belt, which is a ring of icy planetesimals, or comets, which reside beyond the orbit of Neptune [e.g., *Weissman,* 1995]. Within 35-45 AU there are approximately 10^8 to 10^9 comets, and between 45 and 1000 AU there are possibly as many as 10^{13} comets, for a total mass of several hundred Earth masses. This region is vastly unexplored. At the present time only ~60 Kuiper belt objects have been detected by ground-based observatories [e.g., *Brown and Webster,* 1998], and ~13 have been detected by the Hubble telescope [e.g., *Weaver,* 1998].

For optimum scientific return, a spacecraft mission to these regions needs to be performed within a 10 year period after launch. This task is no easy matter. For example, Voyager 1, which was launched in 1977 with a present speed of about 17 km s^{-1} (twice the speed of the space shuttle) is only at ~70 AU and is only expected to reach the termination shock in the next few years. The high speed of Voyager 1 has in part been facilitated by gravitational boosts from its planetary encounters but it is still not expected to cross the heliopause for another 20 years. A 10 year mission to these regions requires a minimum speed of about 50 km/s or equivalently 10 AU yr^{-1}.

A speed of 50 km s^{-1} cannot be easily attained by conventional chemical propellants. The maximum exit velocity from chemical thrusters is only ~3-5 km s^{-1}. To attain speeds above this exit velocity, the fuel-to-payload ratio increases exponentially. Higher propellant velocities can be attained through a variety of plasma devices such as the ion thrusters used on Deep Space 1. The amount of fuel required for such devices is dramatically decreased, but the electrical power requirements would be on the order of megawatts for the speeds being considered here. At this time such power requirements are prohibitively large.

The only other alternative is to tap energy from the ambient medium. One suggested method is the deployment of a solar sail which would produce thrust on the spacecraft through the reflection and/or absorption of solar photons [e.g., *Forward,* 1990]. Proposed solar sails presently consist of a thin film of aluminum with a polymer backing and would provide a sail area of ~4000 to 15,000 m^2 and a net force of 25 to 75 mN. With present technology the sail would have approximately a mass density of about 10 gm/m^2 for a total weight of 40 to 150 kg (with near-future technology developments possibly producing further reductions in weight). Proposals for such solar sails include Mercury Orbiter, where a 500 kg system is proposed to insert a 50 kg payload [*Leipold et al.,* 1995], and the Interstellar Precusor mission [*Mewaldt et al.,* 1999] out to a few hundred AU.

Paper number 1999JA000334.
0148-0227/00/1999JA000334$09.00

Harnessing the energy of the solar wind has also been proposed through the use of magnetic sails or magsail [*Zubrin*, 1993, and references therein]. While different variants have been discussed, the basic concept was to deploy a superconducting magnet with a radius of 100 - 200 km to attain accelerations of the order of 0.01 m s^{-2}. The use of superconducting material would essentially eliminate all power requirements, except for initially setting up the currents and maintaining any cryogenic systems. However, the drawback of such a system was that it was fairly massive (of the order of a few metric tons), and the physical construction and cost of such a system presently limit its usage from technical and/or economic viewpoints.

Mini-Magnetospheric Plasma Propulsion (M2P2) described here is analogous to the solar and magnetic sails in that it seeks to harness ambient energy in the solar wind to provide thrust to the spacecraft. However, it represents major advances in several key areas. First, the M2P2 will utilize electromagnetic processes (as opposed to mechanical structures) to produce the obstacle or sail. Thus the technical and material problems that have beset existing sail proposals are removed from the problem. Second, because the deployment is electromagnetic, large-scale cross sections (15-20 km for a prototype version) for solar wind interactions can be achieved with low weight (<50 kg for the device) and low power (<3 kW) requirements. Third, the M2P2 system acts similarly to a balloon in that it will expand as the solar wind dynamic pressure decreases with distance from the Sun. As such it will provide a constant force surface (as opposed to a mechanical structure that provides a constant area surface) and thereby provide almost constant acceleration to the spacecraft as it moves out into the solar system.

In the following, the physical principles and system requirements are discussed for a spacecraft that could move out of the solar system with speeds of 50–80 km s^{-1} after an acceleration period of about three months. The outline of this paper is as follows. In Section 2, the basic principles and system requirements of the M2P2 system are described. These estimates show that high specific impulse can be attained with existing technology. Detailed numerical results from fluid simulations are presented in section 3, which provide quantitative confirmation of the design concepts. A discussion of possible limitations for the M2P2 is given in section 4 and the results are summarized in section 5.

2. Concept Description

The basic objective of the M2P2 system is to deflect the solar wind particles by a large magnetic bubble whose field lines are attached to the spacecraft. As the charged particles of the solar wind are reflected by the magnetic field, the force that they exert is transmitted along the field lines to the spacecraft to produce its acceleration, as illustrated in Plate 1. In order to produce this coupling the M2P2 system has basically three components: (1) a relatively strong (~700 G) magnetic field on the spacecraft, (2) plasma injected from the spacecraft to inflate the magnetic field, and (3) a power source sufficient to generate the magnetic field and plasma.

The basic problem in coupling to the solar wind is that a current loop by itself can only produce a magnetic field that decreases as R^{-3}. Within ~10 loop radii the magnetic field is essentially zero, and the interaction region with the solar wind is very restricted, and hence inefficient. However, the injection of plasma can drag the magnetic field outward once the plasma moves into a region where the thermal and/or dynamic plasma pressure exceeds the magnetic pressure. As a result the magnetic field can fall off very much more slowly than for a simple dipole, thereby facilitating much more efficient coupling to the solar wind. The exact same processes are responsible for the formation of the heliopause, where solar wind drags or convects magnetic fields from the Sun, which causes the deflection of both the interstellar medium and cosmic rays. Other examples of naturally occurring inflated or stretched magnetic fields include coronal mass ejections and the formation of the Earth's magnetotail.

2.1. Magnetic Field Specification

The magnetic field strength B_{coil} must satisfy two conditions. First, it must be sufficiently strong to ensure that the plasma ions are magnetized, i.e. the width of the plasma source R_{plas} must be at least a few ion gyroradii. Second, the radius of the solenoid R_{coil} must be several times the width of the plasma source to ensure that the ions remain magnetized as they leave the plasma source. Under these conditions, the injected plasma will flow along the field lines until the point is reached where the speed of the plasma V_{plas} matches the local Alfven speed $V_A(x)$. This condition is equivalent to having the dynamic plasma pressure equal to the magnetic pressure (i.e. $\rho V^2 = B^2/\mu_0$). At this point, hereafter referred to as the expansion point R_{expand}, the plasma can drag the magnetic field.

If the plasma were to expand freely at this point, then the magnetic field would decrease as R^{-2}, assuming that the magnetic field is frozen into the plasma. The energy in the injected plasma is sufficient to directly support the increase in magnetic field energy associated with this decrease in falloff. However, the solar wind exerts a force to stop this free expansion and actually does work to stop the sunward flow and drive it backward along the direction of the solar wind flow. As it does so, the injected plasma within the M2P2 is compressed, leading to the formation of current sheets. The magnetic field in the presence of such large-scale current sheets falls off as R^{-1}. As these current sheets are formed, the injected plasma is adiabatically heated (i.e., work is done on the injected plasma by the solar wind), and it is this additional energy that goes to support the slower fall off of the magnetic field. As such the extraction of energy from the solar wind is in two parts: (1) energization of the propellant to higher energies than injected and (2) reflection of the solar wind (as well as the energized injected plasma) off the mini-magnetosphere to propel the spacecraft to higher speeds.

The time-dependent simulations in section 3 quantitatively demonstrate the expansion and its scaling as R^{-1}. The inflation time is seen in the simulations to be ~20 to 50 times the free propagation time and reflects the fact that work needs to done on the injected plasma so that there is sufficient plasma energy to support the current systems within the mini-magnetosphere. The downside of this process is that the injected plasma is energized, and therefore the mini-magnetosphere is subject to the loss of plasma. However, this loss still requires a net reflection of the energetic particles off the magnetic field and so would lead to enhanced propulsion for the spacecraft, albeit not as efficiently as the reflection of solar wind particles. The loss of this plasma at least in the fluid approximation is incorporated in the time-dependent simulations described in the section 3. In the plasma specification derived in section 2.2 we assume 100% loss of plasma injected into the M2P2.

Given the above scheme for the inflation of the M2P2, the magnetic field can be specified as follows. Assuming that the injected plasma starts to drag the field lines very close to the coil (i.e., $V_A(R_{coil})/ V_{plas} \sim 1$), then the relationship between the minimum field strength required to support the system and the system size is given approximately by

$$R_{MP} = (B_{min}/ B_{MP}) R_{coil} \quad (1)$$

where B_{MP}, is the magnetic field strength that is required to deflect the solar wind (i.e., the magnetopause field strength) and

R_{MP} is the distance to the magnetopause along the Sun-satellite line.

For a solar wind density of 6 cm^{-3} and a speed of 450 km s^{-1}, the solar wind dynamic pressure is equivalent to 2 nPa. A magnetic field with B_{MP} = 50 nT is sufficient to produce an equivalent pressure of 2 nPa and hence to be able to deflect the solar wind. In the following we will assume that R_{plas} is 2.5 cm and R_{coil} is 10 cm. For these parameters the minimum coil field strength is about 0.015 T (150 G) in order to produce a mini-magnetosphere of ~15-20 km in size. The total force that would be exerted on such a system would be ~2.5-5 N. As noted above, if $V_A(R_{coil})/V_{plas} > 1$, then the dragging of the magnetic field occurs farther away from the coil where the magnetic field is weaker. In order to produce the same total expansion the field strength at the coil has to be increased. The numerical results suggest empirically that the coil strength has to be increased to

$$B_{coil} \sim [V_A(R_{coil})/ V_{plas}]B_{min} . \quad (2)$$

The field strength for a long solenoid is given by

$$B_{coil} = \mu_0 N I/ L_{coil} \quad (3)$$

where N is the number of turns per unit length, I is the current, and L_{coil} is the length of the coil. The required electrical power is $P_{el} = r_{res} L_{wire} I^2$, where r_{res} is the resistance per unit length of the wire and L_{wire} is the total length of the wire. Thus the relationship between the required electrical power, the coil field strength, and the physical properties of the solenoid is given by

$$P_{el}^{1/2} = (2\pi/\mu_0) B_{coil} r_{res}^{1/2} (L_{coil} R_{coil} / L_{wire}^{1/2}) \quad (4)$$

There is some latitude in choosing the coil parameters depending on whether the main limitation is the weight of the system or the maximum electrical power available. As an illustrative example we will assume that the coil is restricted to a weight of 10 kg. For 10 gauge Al wire, r_{res} = 0.0053 Ω m^{-1} and L_{wire} would be 700 m. While the equivalent Cu wire has lower resistance, it has proportionally more weight, so that Al would be the optimum choice. In this case, (4) reduces to

$$P_{el}^{1/2} = 1.4 \times 10^4 B_{coil} L_{coil} R_{coil} \quad (5)$$

For optimum power considerations, $L_{coil} \sim 2 R_{coil}$, so that for the above parameters only about 16 W would be required to produce B_{min} = 150 G. In reality, $V_A(R_{coil})/ V_{plas}$ is on the order of 5 so that B_{coil} will be ~600 G and the required power would be about 300 W. Less power would be required if there were more weight or, equivalently, L_{wire} were increased. Thus the required magnetic field can be attained with existing technology. Use of superconducting wire can reduce the power requirements albeit at the expense of additional weight.

2.2. Plasma Specification

The inflation of the magnetic field is simplified considerably if the plasma can be produced in the high field solenoidal region of dipole field coils. The plasma will then be magnetized in the field that is to be expanded. For the plasma to stretch the magnetic field the plasma pressure (or, equivalently, energy density) generated by the source must be a nonnegligible fraction of the magnetic field energy. The ratio of these energies is referred to as the plasma β and, as will be shown in section 3.2, an initial β ~1-4 % (or, equivalently, $V_A(R_{coil})/ V_{plas}$ ~ 5-10) in the high field solenoidal region of the dipole field is desired to expand as large a field as possible. For field strengths of the order of 1 kG, a 1% β implies a 5 eV plasma (typical of discharges) and a density of 5 x 10^{13} cm^{-3} (or combination thereof). There are few plasma sources that work in the presence of a strong magnetic field and even fewer capable of producing the high density required. Plasmas generated using electrodes cannot tolerate the high heat load at the high energy densities. There are, however, inductively produced plasma sources (e.g., helicons) that not only produce high-density discharges but do it in the presence of kilogauss magnetic fields.

In existing laboratory helicons the discharges are produced in solenoidal coils with axial fields from a few hundred to 1200 G. The working gas is typically argon, and steady state peak plasma electron densities up to 10^{14} cm^{-3} have been obtained in devices with diameters up to 5 cm [*Miljak and Chen*, 1998; *Gilland et al.*, 1998]. These devices typically use 600 W to 1 kW RF power to produce argon ions and electrons with temperatures of ~4 eV [*Conway et al.*, 1998]. These plasma conditions are equivalent to about ~40 mN of force utilizing ~7.5 x10^{-6} kg s^{-1} or about 0.6 kg day^{-1}. With the bulk speed of the argon being ~3 km s^{-1} these devices produce ~120 W of plasma power. With lighter propellants the mass flux could be reduced to 0.25 kg day^{-1} albeit with an increased energy requirement of ~1 kW.

2.3. Acceleration Period and Spacecraft Speed

The exact final velocity attained by the spacecraft is dependent on the power configuration and the chosen propellant and its mass. For the purpose of the prototype we will assume that the same electrical power is available as for Deep Space 1, i.e., 2.5 kW at 1 AU. If a light propellant is used, then the spacecraft can move out to R_{cutoff} = 1.4 AU before the electrical power falls below that required by the M2P2 system to operate. Beyond R_{cutoff} the M2P2 system has to be run in pulsed mode with a duty cycle of $(R_{cutoff}/R)^2$.

The acceleration curves are shown in Figure 1 for the M2P2 system assuming that R_{cutoff} = 1.4 AU and that 1 N of force from the solar wind is intercepted. Two cases are shown: case A, in which the spacecraft has 100 kg mass (70 kg payload and 30 kg propellant), and case B in which the spacecraft mass is 200 kg (170 kg payload and 30 kg propellant). In the two cases, speeds of 50 to 75 km s^{-1} are attained. These speeds are well above anything that has previously been flown.

The restriction on the available power is the main limitation to the spacecraft speed. If the solar electric cells were supplemented by some form of radioactive isotope power system (100 W), which would be required for any type of deep-space communication system then the M2P2 system could be run in pulsed mode for several tens of AU. In this case, speeds of nearly 100 km s^{-1} could be attained.

3. Multi-Fluid Simulations

Sections 2.1-2.2 show that the inflation of the M2P2 system is technically feasible with all of the enabling technology readily available at this time. In this section we use time-dependent multi-fluid simulations to show that the M2P2 system can be inflated with the injection of low-energy plasma and produce the required deflection of the more energetic solar wind plasma at distances very much larger than would be expected from a simple dipole magnetic field. The three-dimensional (3-D) simulations are also important because, in the calculations in section 2, essentially all the plasma is assumed to be lost. Thus the fuel consumption rates in section 2 represent a maximum estimate. The 3-D simulations incorporate losses from the mini-magnetosphere due to (1) leakage of plasma across the magnetopause and/or (2) convection of plasma downstream into the tail of the mini-magnetosphere.

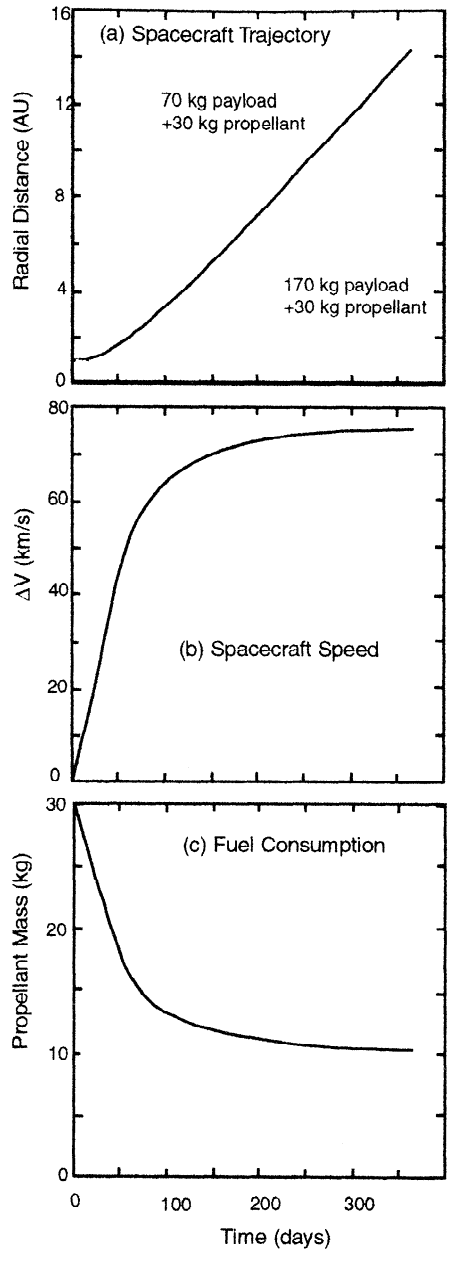

Figure 1. The trajectory, speed, and fuel consumption for the M2P2 system assuming 1 N of force from the solar wind, a fuel consumption of 0.25 kg s^{-1} when the device is on, and a R^{-2} decrease in power with R_{cutoff} = 1.4 AU.

These simulations show that the estimates in Section 2 for the force needed to sustain the mini-magnetosphere are actually overly pessimistic and that as little as a few millinewtons of force are required to sustain the system and intercept a force of ~1 N from the solar wind. This leverage of force is the innovative feature of the M2P2 system, and it is key to producing high-speed acceleration of the spacecraft with very modest power and mass requirements.

The numerical model is the same as that used by *Winglee* [1998a, b] for modeling the terrestrial magnetosphere (earlier versions as applied to the magnetosphere and to the formation of stellar jets are given by *Winglee et al.* [1996] and *Goodson et al.* [1997], respectively). A multi-fluid treatment is used so that the dynamics of the solar wind plasma can be separated from the dynamics of the injected plasma inflating the magnetosphere. While the overall configuration is very similar to that derived from single-fluid MHD, the multi-fluid treatment enables the change in momentum due to the deflection of the solar wind by the magnetic barrier to be explicitly calculated. Thus, the net force on the spacecraft can be determined from the simulations by conservation of momentum.

3.1. Numerical Algorithm

MHD is based on the fluid equations for plasmas, but the equations for conservation of mass and energy are combined to give a single-fluid treatment. Our multi-fluid treatment is based on the same equations, but the dynamics of the electrons in the different ion species are kept separate. Specifically for electrons, it is issued that they have sufficiently high mobility along with the lines such that they are approximately in steady state (i.e. $d/dt = 0$) or have drift motion, so that the momentum equation for the electrons reduces to

$$\mathbf{E} + \frac{\mathbf{V_e} \times \mathbf{B}}{c} + \frac{\nabla P_e}{e n_e} = 0 \tag{6}$$

Equation (6) is equivalent to the modified Ohm's law with Hall and grad P corrections included. The rest of the electron dynamics is given by assuming quasi-neutrality and applying the definitions for current and electron pressure, i.e.,

$$n_e = \sum_i n_i, \quad \mathbf{V_e} = \sum_i \frac{n_i}{n_e}\mathbf{V_i} - \frac{\mathbf{J}}{e n_e}, \quad \mathbf{J} = \frac{c}{4\pi}\nabla \times \mathbf{B} \tag{7}$$

$$\frac{\partial P_e}{\partial t} = -\gamma \nabla \cdot (P_e \mathbf{V_e}) + (\gamma - 1)\mathbf{V_e} \cdot \nabla P_e \tag{8}$$

Substituting the modified Ohm's law (6) for the electric field into the ion momentum equation yields

$$\rho_\alpha \frac{dV_{\|\alpha}}{dt} = -(\nabla P_\alpha)_\| - \frac{n_\alpha}{n_e}(\nabla P_e)_\| \tag{9}$$

$$\rho_\alpha \frac{dV_{\perp\alpha}}{dt} = e n_\alpha \left(\frac{\mathbf{V_\alpha} \times \mathbf{B}}{c}\right) - \sum_i \frac{n_i}{n_e}\frac{\mathbf{V_i} \times \mathbf{B}}{c} + \frac{n_\alpha}{n_e}\left[\frac{\mathbf{J} \times \mathbf{B}}{c} - (\nabla P_e)\right]_\perp - (\nabla P_\alpha)_\perp \tag{10}$$

where the $\|$ and $\perp$ subscripts indicate components parallel and perpendicular to the magnetic field, respectively. For plasmas with a single ion component, (10) reduces to the MHD momentum equation.

To remove high-frequency cyclotron oscillations, the different ion species are assumed to have the same drifts across the field line, i.e.,

$$\mathbf{V}_\perp = \sum_i \rho_i \mathbf{V}_{\perp i} / \sum_i \rho_i \tag{11}$$

This approximation is the same as assumed in MHD and allows the perpendicular ion momentum to be simplified to

$$\sum_\alpha \rho_\alpha \frac{dV_{\perp\alpha}}{dt} = \left[\frac{\mathbf{J} \times \mathbf{B}}{c} - (\nabla P_e)_\perp\right] - \sum_\alpha (\nabla P_\alpha)_\perp \tag{12}$$

$$\frac{\partial P_\alpha}{\partial t} = -\gamma \nabla \cdot (P_\alpha \mathbf{V_\alpha}) + (\gamma - 1)\mathbf{V_\alpha} \cdot \nabla P_\alpha \tag{13}$$

The above equations are solved using a two-step Lax-Wendroff differencing scheme [*Richtmyer and Morton*, 1967] with Lapidus smoothing on plasma properties only. The latter is required to remove nonphysical grid point oscillations across sharp discontinuities such as the bow shock.

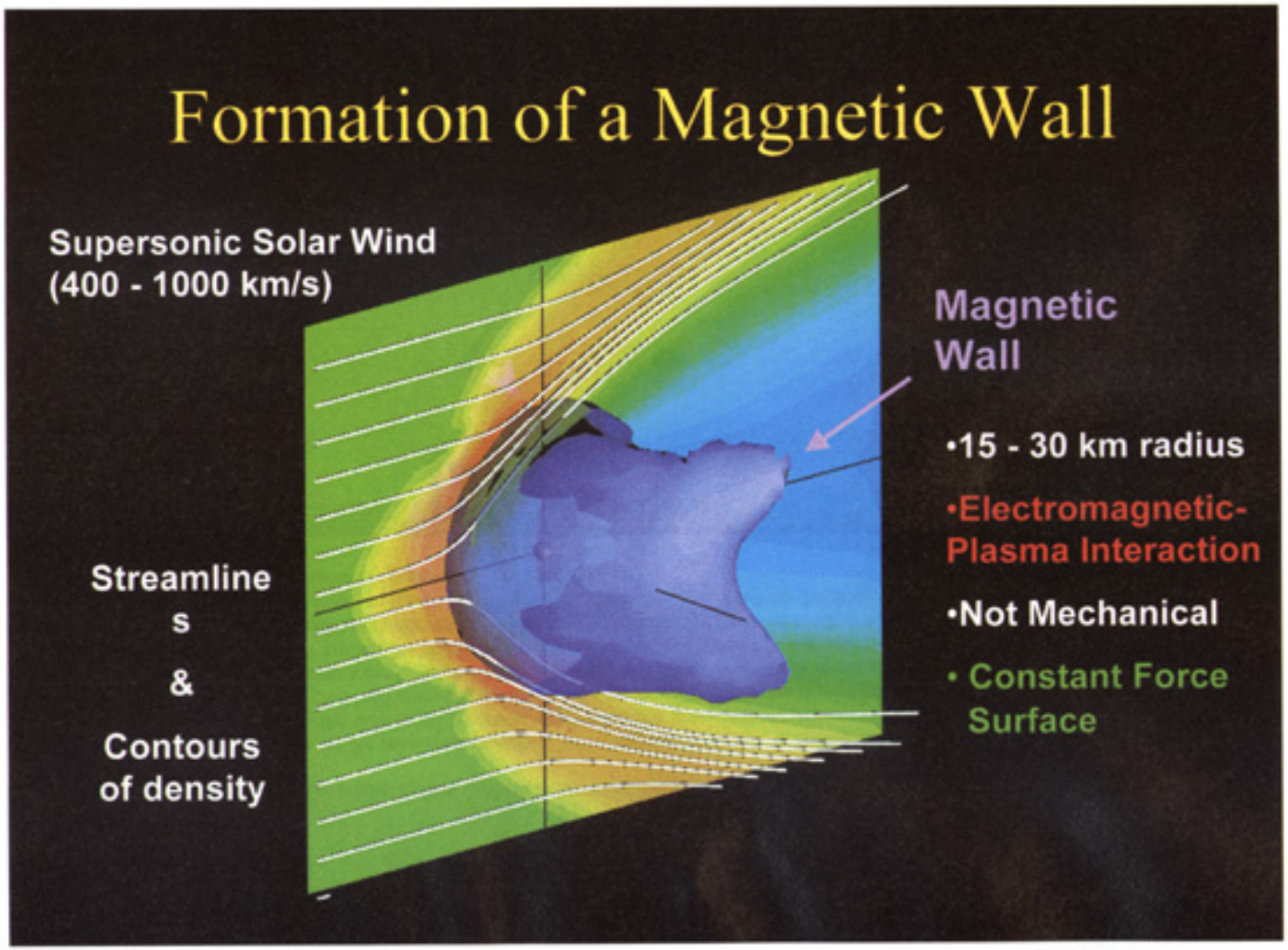

Plate 1. Schematic (based on simulations results) showing the deflection of the solar wind by a magnetic wall or mini-magnetosphere. Plasma is injected into a moderately strong magnetic field supported by field coils on the spacecraft. The injection produces the inflation of the magnetic field to form the mini-magnetosphere. This magnetic field is able to deflect the solar wind particles with speeds of 400–1000 km s^{-1}, as seen by the white streamlines. The color contours display plasma density with red indicating the pileup of solar wind plasma. The size of the system is determined by pressure balance between the M2P2 system and the solar wind dynamic pressure: It is not limited by mechanical structures.

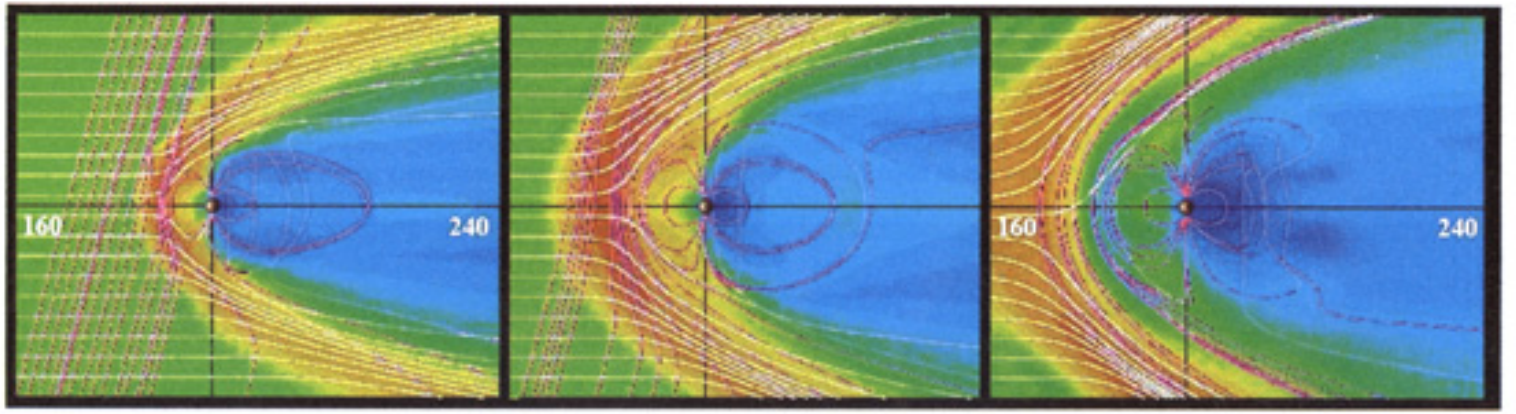

Plate 2. Inflation on the mini-magnetosphere when the magnetic axis is orthogonal to the solar wind flow. Color contours indicate the density of the solar wind, with the green regions representing the undisturbed solar wind density of 6 cm^{-3}, red indicating enhancements of a factor of 4 as solar wind piles up around the magnetopause, and blue regions indicating depleted density in the wake with densities as small as 0.1 cm^{-3}. White lines show the flow of the solar wind around the mini-magnetosphere while magenta lines indicate the magnetic field lines. Only a subset of the simulation system is shown for clarity, extending 160 times the spacecraft (which is represented by a sphere of 5 grid units) on upstream side and 240 times the spacecraft on the downstream side. The brown sphere (not to scale) indicates the position of the spacecraft.

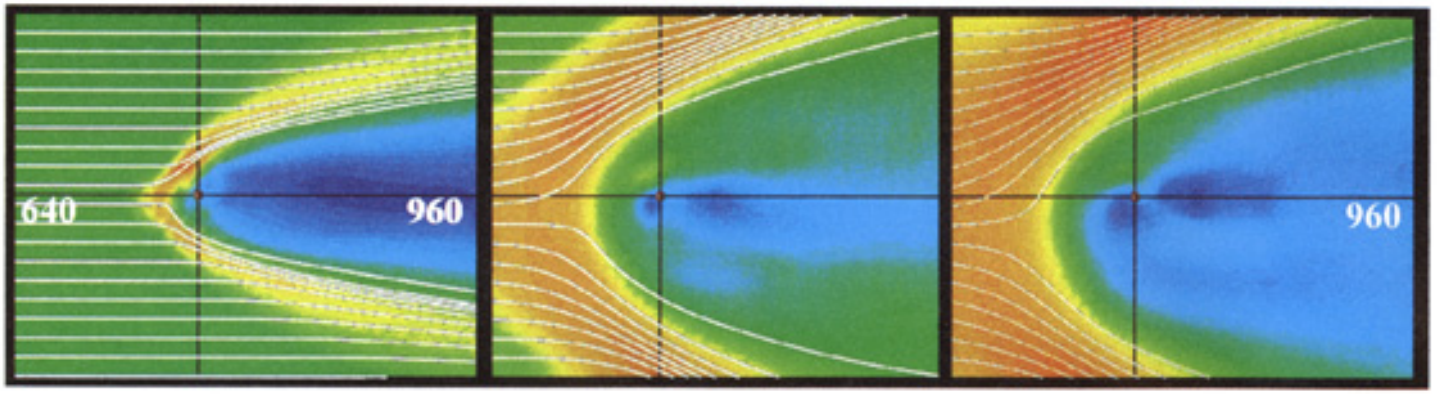

Plate 3. As in Plate 2, except that the dipole has an orientation of 45° and the system size is four times larger in each direction (i.e., 640 times the inner radius on the dayside to 960 spacecraft radii on the nightside). The initial configuration is the same as the right diagram of Plate 2, but because of the change of scale the mini-magnetosphere appears smaller. As the magnetic field strength and the density of the injected plasma are increased, the mini-magnetosphere is again seen to expand. In addition, because of the tilting of the dipole, the flow lines preferentially pass over the top of the mini-magnetosphere, and the spacecraft would experience azimuthal as well as radial acceleration.

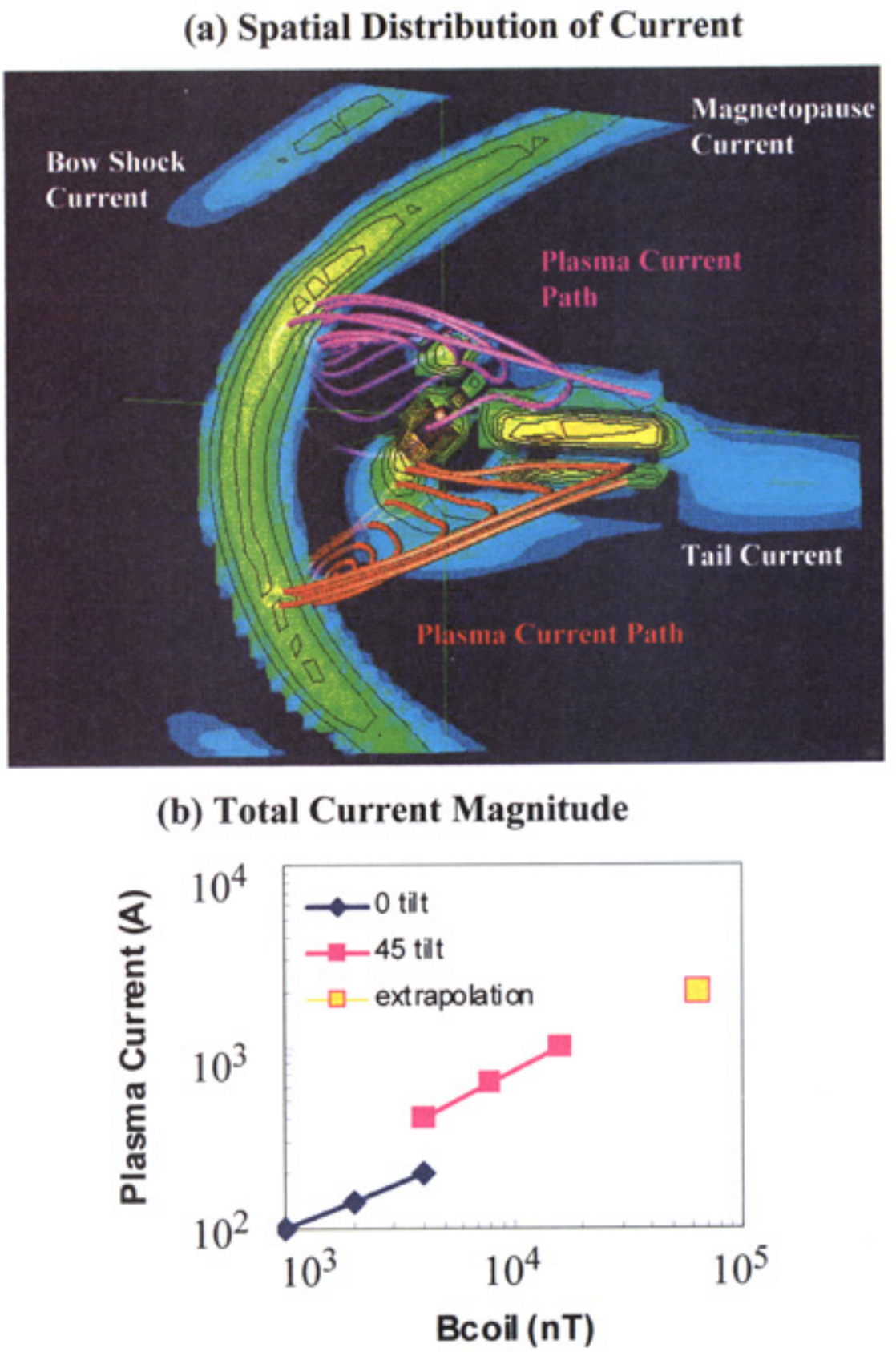

Plate 4. (a) Three-dimensional (3-D) rendering of the induced plasma current system. Contours indicate intensities in the *x-z* plane while the lines show the current path in 3-D for two sample regions. (b) The total induced current as a function of the coil field strength. For the M2P2 system several to a few tens of kiloamps will be generated.

The most difficult part of simulations is in trying to get realistic scaling since the expansion produces interactions over scale sizes 10^5 larger than the spacecraft itself. In terrestrial magnetospheric models the bow shock is within ~13-15 R_E (where 1 R_E is the Earth radius), and the inner radius of the simulations is typically 3 R_E, so that the change in scale is very much smaller. While the simulations cannot handle a 10^5 change in scale lengths, they can treat a factor of 10^3 (this dynamic range is orders of magnitude larger than existing global simulation models of the terrestrial magnetosphere). This large range of scales is treated in the simulations by breaking the grid system up into a series (nine in all) of subsystems where the grid spacing increases by a factor of 2 between consecutive subsystems. The smaller subsystem provides the inner boundary conditions for the next larger subsystem, and, conversely, the larger subsystem provides the outer boundary conditions for the smaller subsystem. This nesting of subsystems allows us to have high spatial resolution around the spacecraft while still allowing resolution of the reflection of the solar wind particles at the bow shock of magnetosphere to be fully resolved.

In the simulation results presented, the subsystems consist of 50 x 40 x 40 grid points with the spacecraft being represented by a sphere with a radius a 5 grid points. In principle the simulation results can be scaled to arbitrarily large or small systems so long as the fluid approximation is valid; that is, the gyroradius of an ion in the dipole magnetic field must be smaller than the scale length of the dipole. For simplicity of scaling the results to a spacecraft system, the results are placed in absolute units assuming that the largest subsystem represents 10 km and the inner radius represents a 10 m region around the spacecraft with a grid resolution of 2 m around it. For the lower values of field strength assumed here, the fluid approximation is only marginally met at best, and, strictly speaking, the simulations would have to represent systems of larger scale lengths. They are included so that the extent of the scaling can be more clearly seen.

The solar wind is assumed to have nominal values of 500 km s^{-1} and density of 6 cm^{-3} while the spacecraft is assumed to have initially only a weak (1000 nT) magnetic field. The simulations are then run for about four transit times (0.4 s), thereby enabling solar wind to come into an approximate equilibrium with the formation of the spacecraft shock wave and wake.

Once this equilibrium has been established, the magnetic field strength is doubled, and the plasma injection begins with a speed of 20 km s^{-1} such that V_A / V_{plas} = 5. The solar wind is then allowed to come into a new equilibrium. The size of the mini-magnetosphere and the change it produces in the solar wind momentum are then calculated from the simulations. The process is repeated by increasing the magnetic field and the plasma density by factors of 2 and 4, respectively, so that V_A / V_{plas} remains constant. In this manner we can thereby determine the scaling of the size of the mini-magnetosphere as a function of the solenoid field strength.

3.2. Numerical Results

Plate 2 shows the change in size of the mini-magnetosphere for B_{coil} equal to 1000, 2000 and 4000 nT (Plate 2, left, middle, and right, respectively). For the weak magnetic field in Plate 2, left, the bow shock and magnetopause are relatively close to the spacecraft. With a doubling of the magnetic field strength and associated plasma injection on the spacecraft, both the bow shock and magnetopause are seen in Plate 2, middle, to be pushed outward, almost doubling the distance. Increasing the magnetic field strength by a further factor of 2 creates another approximate doubling of the system (Plate2, right).

These results are suggestive that the scale size of the M2P2 is directly proportional to the strength of the magnetic field as suggested in section 2. A test of this hypothesis is shown in Plate 3, where the solar wind profile is plotted on a scale size 4 times larger and where the magnetic field strength is increased by a factor of 4 from the left to right diagrams of Plate 3. For greater clarity the field lines have been removed. The positions of the magnetopause and bow shock push out approximately by the expected factor of 4.

One difference between Plates 3 and 2 is that the magnetic dipole is tilted by 45° into the solar wind. One of the main effects of this tilting is that the streamlines initially below the equator are deflected so that they pass over the spacecraft. As a result there is a net azimuthal acceleration on the M2P2. In other words, the M2P2 system is not just a drag device, but lift or azimuthal acceleration can be obtained as with an ordinary solar sail by tilting the dipole.

The results of Plates 2 and 3 are summarized in Figure 2. The standoff distance, or equivalently, the distance to magnetopause along the Sun-spacecraft line, shows more than an order of magnitude increase as the magnetic field is increased by a factor of ~20. The distance is also nearly an order of a magnitude greater than could be expected for the solar wind interaction with a simple dipole with no plasma injection. Note also that the standoff distance is used here since it is the simpler measurement, irrespective of the orientation of the dipole. However, the standoff distance is ~30% smaller than the radial cross-sectional distance. Extrapolating along the curve, the magnetic field strength that is required to produce a 15 km standoff distance (or 20 km cross-sectional distance) is ~6-7 G for our 10 m inner radius. Scaling this to a 0.1 m radius would imply that we need a magnetic field of 600-700 G on the spacecraft coils.

A second effect of tilting the magnetic axis into the solar wind is that the magnetosphere that is produced is actually larger. This increase in size is due to the stronger magnetic fields at the poles. The implication is that the configuration in which the magnetic axis is orthogonal to the solar wind direction is the lowest energy state and there is no danger of the solar wind blowing the M2P2 over and causing it to lose its effectiveness. Thus higher thrust would be attainable if the dipole axis were tilted toward the solar wind, but some additional propellant would have to be expended in order to maintain its orientation.

The total force that is imparted onto the M2P2 is shown in Figure 3. This force is calculated from the simulations using the net change in the momentum flux in the solar wind plasma upstream of the M2P2 integrated through the *y-z* plane containing the spacecraft. There is additional force exerted on the spacecraft from the tail, so the estimates described here represent a lower limit. Conservation of momentum requires that this momentum flux must be picked up by the spacecraft. It is seen that the M2P2 gives substantial leverage or multiplication factor between the force required to sustain the M2P2 and the force exerted on the spacecraft by the solar wind. Extrapolation of the simulation results indicates that in order to gain the 1 N of force on the spacecraft only ~3 mN have to be expended for a leverage of between 300 and 400.

An alternative way to look at the force on the M2P2 system is through the equivalent current system produced by the solar wind interaction with the mini-magnetosphere, as illustrated in Plate 4. There are two current systems involved. The first consists of the current loops on the spacecraft that support the dipole-like magnetic field. The injection of plasma produces the second current system in space, similar to the terrestrial current system. These plasma currents are strongest around the magnetopause and are closed by currents near the spacecraft as indicated by the line traces along the current paths.

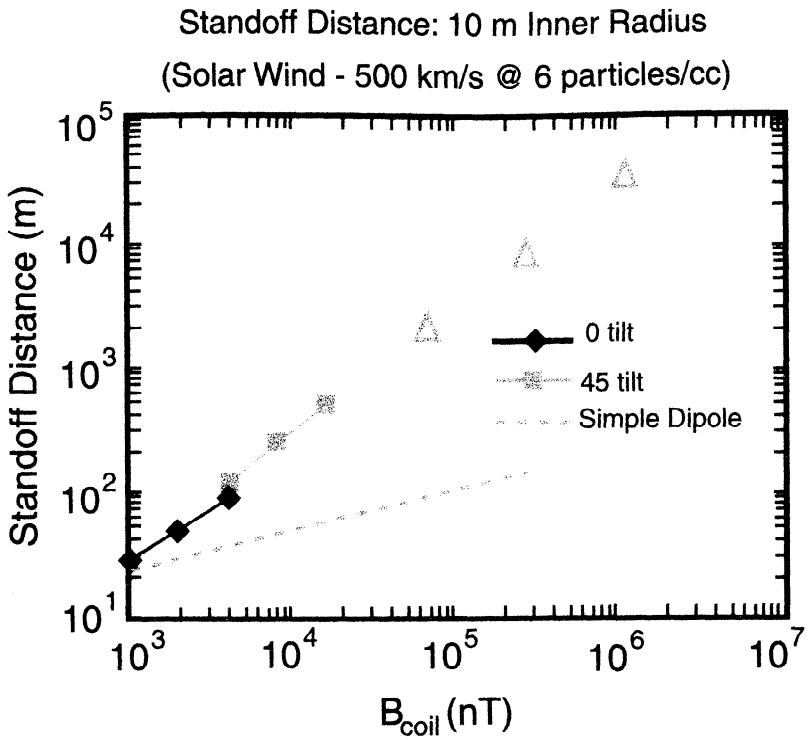

Figure 2. Size of the mini-magnetosphere as a function of coil field strength (and density of the injected plasma) for V_A / V_{plas} = 5 as given by the distance between the spacecraft and the magnetopause along the Sun-spacecraft line. The size of the inflated magnetopause is very much larger than a simple dipole, increasing almost linearly with field strength. The triangles represent an extrapolation of the simulation results to approximately the regime in which the M2P2 would be operated.

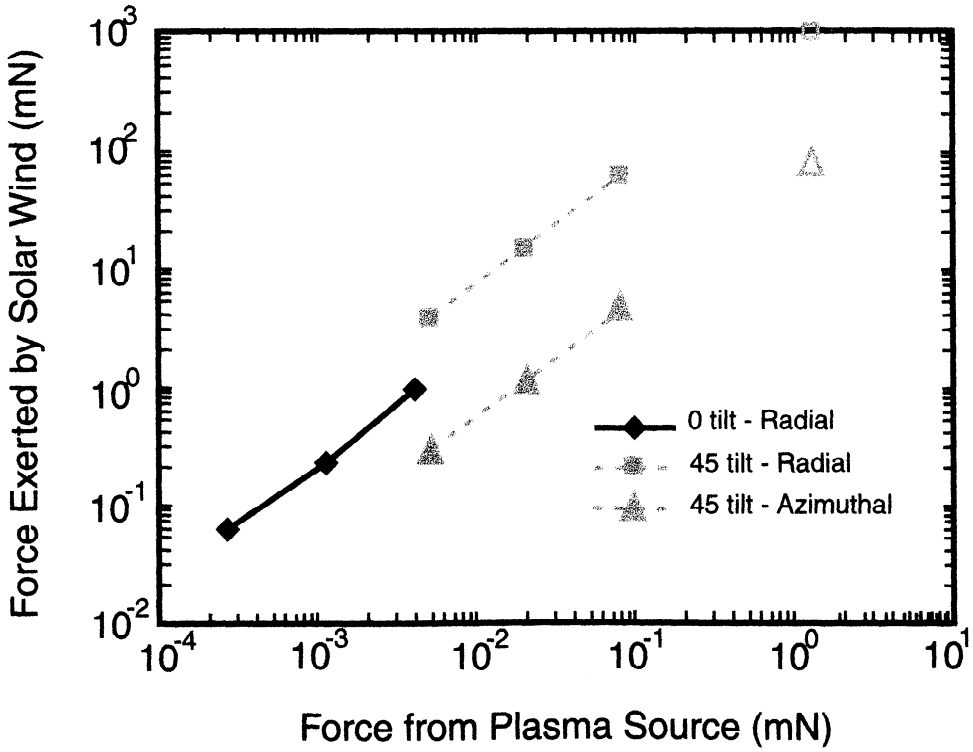

Figure 3. Force developed on the M2P2 system derived from the simulations. The triangles indicate an extrapolation to the regime for the efficient operation of the M2P2. Because the inflation is produced by injection of low-energy plasma, there is a substantial leverage of force between that required to inflate the M2P2 system and that exerted on it by the solar wind. The simulations indicate that only a few millinewtons of injected plasma are required to intercept 1 N of force from the solar wind. The force is more than enough to overcome the solar gravitational force which at 1 AU is 0.6 N on 100 kg.

These current paths are "D"-shaped. In the absence of outside forces the current paths should be circular. Compression into a "D" is due to the force exerted by the solar wind, which is trying to pick up the plasma current system, as it would with any plasma turbulence, and convect it downstream. As it does so, the plasma currents feel the force from the spacecraft magnetic coils, and vice versa, producing the acceleration on the spacecraft. The simulations show that several kiloamps of current will be induced by the M2P2 system. The current on the spacecraft, while only ~10 A, is driven through ~1000 turns and therefore represents a comparable system, so that the two systems are capable of producing a force of about a newton on each other.

4. Potential Limitations

The main uncertainty for the viability of the M2P2 system is whether the plasma losses will be too large to allow efficient coupling to the solar wind. The results presented in section 3 represent a fluid treatment, and as such, only fluid instabilities are incorporated. The main loss mechanism in this fluid approach is via convection and is taken into account in the estimates for fuel consumption rate of the M2P2. Wave-particle interactions are not included but could be an important mechanism for heating of the particles and enhancing the loss rate from the mini-magnetosphere above that presently calculated. Treating these wave-particle interactions is beyond the scope of this paper. However, the following comments can be made about particle losses from the system.

The time-dependent simulations presented here suggest that the M2P2 is stable to (i.e. not disrupted by) macroscopic fluid instabilities such as the interchange and ballooning instabilities. The absence of these instabilities is in part due to the dipole geometry and because the plasma β is only of order unity and insufficient to drive these instabilities. This stabilization appears to be consistent with recent calculations for dipole confinement in laboratory plasmas [*Kesner and Mauel,* 1997; *Garnier et al.,* 1999].

The development of kinetic instabilities, while probable, is not necessarily catastrophic to the overall stability of the mini-magnetosphere for three reasons. First, the electrons are strongly bound to the field lines, and kinetic instabilities are unlikely to effectively scatter the electrons off the field lines. Because the density is much larger than the solar wind density, quasi-neutrality requires that the bulk of the ions remain tied to the field lines. Second, the ions that are lost would effectively be scattered from strong magnetic field into low magnetic field regions. Thus there would be a net gain of momentum on the magnetic field coils as these particles are lost. Since this loss mechanism is most likely to occur for high-energy particles, there is still an energy leverage between that used to inflate the magnetosphere and that which is being reflected off it. Third, mini-magnetospheres of the same scale size (~100 km) have been observed on the Moon by Lunar Prospector [*Lin et al.,* 1998], and while these mini-magnetospheres are clearly turbulent, surface field strengths of ~300 nT are sufficient to macroscopically cause the pileup and deflection of solar wind plasma at least to the 100 km altitude of Lunar Prospector.

Another loss mechanism for the M2P2 is through reconnection. This process is included in the multi-fluid simulations. If the IMF is antiparallel to the dipole field, there is enhanced convection of plasma down the tail of the mini-magnetosphere in much the same way as the terrestrial magnetosphere responds to southward interplanetary magnetic field (IMF). However, the cross section of the magnetosphere in this case is larger than for the parallel configuration. Thus if power as opposed to fuel is the greatest restriction on spacecraft, then an antiparallel configuration would be the most advantageous. Conversely, if fuel is the primary concern, then a parallel configuration could be the more appropriate one. Note though that these IMF modulations represent only a change in force of ~10-20% of the total force exerted on the M2P2 since the solar wind in general has a high Mach number (i.e., the solar wind dynamic pressure is much larger than the magnetic energy density in the IMF).

Variations in the solar wind dynamic pressure are not expected to have a serious disrupting effect on the M2P2 because it acts like a constant force device. Specifically, the fundamental principle of the mini-magnetosphere is that it is in pressure equilibrium with the solar wind. Thus if the solar wind dynamic pressure increases, for example, because of the presence of a magnetic cloud, the mini-magnetosphere will be compressed, and its cross section will be decreased. Conversely, if the solar wind dynamic pressure decreases, the mini-magnetosphere will expand correspondingly. Such compression and expansion are seen even in the terrestrial magnetosphere. This effect has a major advantage for the M2P2, in that as a spacecraft moves out of the solar system and the solar wind dynamic pressure decreases, the spacecraft, assuming that the electrical power can be maintained, could potentially experience an almost constant acceleration out to 80 AU. For mechanical sail the cross-sectional area is fixed, and the force will fall off as R^{-2}.

5. Summary

In order to explore the outer solar system and nearby interstellar space, spacecraft will have to travel at speeds in excess of 50 km s^{-1}. The power requirements needed to obtain such high speeds are much higher than can be presently supported by solar electric propulsion. Thus some other means for powering the spacecraft must be developed. In this paper we have investigated one such system, where energy from the solar wind is used to propel the spacecraft. This system, which we call Mini-Magnetospheric Plasma Propulsion (M2P2), seeks to inflate a large magnetic bubble around the spacecraft to deflect and thereby pick up the momentum from the solar wind particles, which are traveling at speeds of 350 to 800 km s^{-1}.

The M2P2 system, which in its simplest form will enable the spacecraft to attain speeds of 50 to 80 km s^{-1}, has several advantageous features. First, inflation of the magnetic bubble is done electromagnetically through the injection of plasma, so that technical and material problems associated with the deployment of large mechanical structures are eliminated. Second, very large cross sections (15–20 km) can be achieved with minimal mass (<0.5 kg per day) and power requirements (<1 kW). The bubble produced in this way requires a few millinewtons of force from the injected plasma to maintain the bubble while experiencing a force of the order of 1 N from the solar wind. This leverage in force is attained because the solar wind has a speed very much higher than the plasma being injected from the spacecraft.

The third feature of the M2P2 system is that the mini-magnetosphere acts very much like a bubble in that it will expand as a spacecraft moves out of the solar system to match the decline in the solar wind dynamic pressure. This means that if some form of radioactive isotope power system were available to supplement the electrical power even at, say, 100W, the M2P2 system could be run in pulsed-mode operation to provide continuous acceleration of the spacecraft as it moves into the outer solar system. Such an auxiliary power system could allow speeds of ~100 km s^{-1} to be obtained. Continuing research at the University of Washington seeks to build and test a prototype in laboratory for its eventual deployment in space.

Acknowledgments. This work was supported by a grant from NASA's Institute for Advance Concepts 07600-010, NSF grant ATM-9731951, and NASA grants NAG5-6244, and NAG5-8089 to the

Univeristy of Washington. The simulations were supported by the Cray T-90 at the San Diego Supercomputing Center, which is supported by NSF.

Janet G. Luhmann thanks Gerhard Haerendel and two other referees for their assistance in evaluating this paper.

References

Baranov, V. B., and Y. G. Malama, Model of the solar wind interaction with the local interstellar medium: Numerical solution of the self-consistent problem, *J. Geophys. Res., 98*, 15,157, 1993.

Baranov, V. B., and Y. G. Malama, Effect of local interstellar medium hydrogen fractional ionization on the distant solar wind and interference region, *J. Geophys. Res., 100*, 14,755, 1995.

Brown, M. J. I., and R. L. Webster, A search for bright Kuiper belt objects, *Proc. Astron. Soc. of Aust., 15*, 176, 1998.

Conway, G. D., A. J. Perry, and R. W. Boswell, Evolution of ion and electron energy distributions in pulsed helicon plasma discharges, *Plasma Sources Sci. and Technol., 7*, 337, 1998.

Forward, R. L., Grey solar sails, *J. Astron. Sciences, 38*, 161, 1990.

Garnier, D. T., J. Kesner, and M. E. Mauel, Magnetohydrodynamic stability in a levitated dipole, *Phys. Plasmas, 6*, 3431, 1999.

Gilland, J., R. Breun, and N. Hershkowitz, Neutral pumping in a helicon discharge, *Plasma Sources Sci. Technol., 7*, 416, 1998.

Goodson, A. P., R. M. Winglee, and K.-H. Bohm, Time dependent accretion of magnetic young stellar objects as a launching mechanism for stellar jets, *Astrophys. J., 489*, 199, 1997.

Kesner, J., and M. Mauel, Plasma confinement in a levitated magnetic dipole, *Plasma Phys. Rep., 23*, 742, 1997.

Leipold, M., E. Borg, S. Lingner, A. Pabsch, R. Sachs, and W. Seboldt, Mercury orbiter with a solar sail spacecraft, *Acta Astronaut., 35*, 635, 1995.

Lin, R. P. et al., Lunar surface magnetic fields and their interaction with the solar wind: results from Lunar Prospector, *Science, 281*, 5382, 1998.

Linde, T. J., T. I. Gombosi, P. L. Roe, K. G. Powell, and D. L. DeZeeuw, Heliosphere in the magnetized local interstellar medium: Results of a three-dimensional MHD simulation, *J. Geophys. Res., 103*, 1889, 1998.

Mewaldt, R. A., P. C. Liewer, and S. A. Gavit, An interstellar probe to the boundaries of the heliosphere and nearby interstellar space, *Eos Trans., AGU, 80*(17), Spring Meet. Suppl., S237, 1999.

Miljak, D. G., and F. F. Chen, Density limit in helicon discharges, *Plasma Sources Sci. and Technol., 7*, 537, 1998.

McComas, D. J., S. L. Bame, B. L. Barraclough, W. C. Feldman, H. O. Funsten, J. T. Gosling, P. Riley, and R. Skoug, Ulysses' return to the slow solar wind, *Geophys. Res. Lett., 25*, 1, 1998.

Richtmyer, R. D., and K. W. Morton, *Difference Methods for Initial Value Problems*, pp. 300, Interscience, New York, 1967.

Steinolfson, R. S., V. J. Pizzo, and T. Holzer, Gasdynamic models of the solar wind/interstellar medium interaction, *Geophys. Res. Lett., 21*, 245, 1994.

Suess S.T., The heliopause, *Rev. Geophys., 28*, 97, 1990.

Weaver, H. A., Comets, in *The Scientific Impact of the Goddard High Resolution Spectrograph (GHRS)*, editd by J. C. Brandt, T. B. Ake III, and C.C. Peterson, *Astron. Soc. Pac. Conf. Ser., 143*, pp. 213-226, 1998.

Weissman, P. R., The Kuiper belt, *Annu. Rev. Astron. Astrophys., 33*, 327, 1995.

Winglee, R. M., Multi-fluid simulations of the magnetosphere: The identification of the geopause and its variation with IMF, *Geophys. Res. Lett., 25*, 4441, 1998a.

Winglee, R. M., Imaging the ionospheric and solar wind sources in the magnetosphere through multi-fluid global simulations, *Phys. Space Plasmas, 15*, 345, 1998b.

Winglee, R. M., et al., Modeling of upstream energetic particle events observed by WIND, *Geophys. Res. Lett., 23*, 12,276, 1996.

Zubrin, R. M., The use of magnetic sails to escape from low Earth orbit, *J. Br. Interplanet. Soc., 46*, 3, 1993.

A. Goodson, The Boeing Corporation, P. O. Box 3999, MS 84-33, Seattle, WA 98124. (Anthony.Goodson@PSS.Boeing.com.)

J. Slough and T. Ziemba, Department of Aeronautics and Astronautics, Box 352250, University of Washington, Seattle, WA 98195-2250.(slough@aa.washington.edu; tim@aa.washington.edu.)

R. M. Winglee, Geophysics Program, Box 351650, University of Washington, Seattle, WA 98195-1650. (winglee@geophys.washington.edu.)

(Received September 10, 1999; revised December 29, 1999; accepted January 26, 2000.)